



Catalytic activity of synthesized nanosized molybdenum disulfide for the hydrodesulfurization of dibenzothiophene: Effect of H₂S partial pressure

Hamdy Farag^{a,*}, Abdel-Nasser A. El-Hendawy^b, Kinya Sakanishi^c, Masahiro Kishida^a, Isao Mochida^d

^a Department of Material Process Engineering, Graduate School of Engineering, Kyushu University, Motooka 744, Fukuoka 819-0395, Japan

^b Physical Chemistry Department, National Research Center, 12622 Dokki, Cairo, Egypt

^c Biomass Technology Research Center, AIST, Kure, Hiroshima 737-0197, Japan

^d Institute for Materials Chemistry and Engineering, Kyushu University, Fukuoka 816-8580, Japan

ARTICLE INFO

Article history:

Received 17 April 2009

Accepted 20 May 2009

Available online 27 May 2009

Keywords:

MoS₂

Hydrodesulfurization

Dibenzothiophene

H₂S

ABSTRACT

Nanosized MoS₂ catalysts with basal planes of ~4 nm were synthesized by thermally annealing ammonium tetrathiomolybdate. The structure and morphology of the obtained phases were determined by XRD, SEM and TEM. These nanosized MoS₂ clusters have a truncated hexagonal shape. The MoS₂ layers in these batches were found to be curved to some extent. Catalytic performance was evaluated by the hydrodesulfurization of dibenzothiophene. We studied the effect of a wide range of H₂S partial pressures on the hydrodesulfurization activity and selectivity. Catalytic activity for the hydrodesulfurization of dibenzothiophene increased remarkably when H₂S was included within the reaction zone. The role of the curved MoS₂ layers on activity is discussed.

© 2009 Elsevier B.V. All rights reserved.

1. Introduction

Transition metal sulfides are a class of material that have many interesting properties in several areas of materials application such as in catalysis [1], semiconductor technology [2], lubrication [3,4], sensing [5,6] and hydrogen storage [7]. The unique structures of these materials have led to various studies. These materials are the backbone catalysts in petroleum refineries where they are widely adapted for many refining stages. Molybdenum disulfide is one of these interesting materials and has shown the ability to catalyze many reactions such as hydrodesulfurization [1] and synthesis gas reactions [8]. It comprises stacked layers in which each layer consists of a molybdenum layer sandwiched between two sulfide layers. The layers are bound by van der Waals forces which are weak enough to allow the layers to move back and forth if exposed to any external strain. This property has enabled the molybdenum disulfide to serve as an efficient lubricant. This texture of the molybdenum disulfide is also of importance in its catalytic performance. Regardless of the method of molybdenum disulfide synthesis, the product stoichiometry is mostly identical, however, its textural characteristics are many and varied. Small differences

may be found in the morphology and in the atomic structure of the layers.

In a previous study [9], the precursor and the implemented heat treatment played key roles in controlling the obtained particle size and thus the morphology of the molybdenum disulfide product. Selectivity during hydrodesulfurization of model sulfur compounds has been shown to be dependent on the MoS₂ crystallite size. Inhibition and/or promotion of catalytic activity of MoS₂ by H₂S in the hydrodesulfurization reaction have been found to be partially dependent on the crystallite size [10,11]. Recently [12–17], bulk transition metal sulfides have been shown to have interesting hydrotreating activities and the NEBULA catalyst series, for instance, was claimed to have efficient performance for many hydrotreating operations [18]. The structure of the nanosized bulk molybdenum sulfide must be important because it was linked to catalytic performance. Studying the behavior and performance of nanosized MoS₂ particles may provide a crucial clue to explain the performance of the based catalysts. Reaction inhibition and/or promotion by H₂S during hydrodesulfurization (HDS) over MoS₂ is very sensitive to the catalyst's particle size.

In this study, we investigated the HDS of dibenzothiophene (DBT) over a nanosized molybdenum disulfide catalyst that was derived from ammonium tetrathiomolybdate. The performance of this catalyst in DBT HDS reactions under different partial pressures of H₂S was emphasized. This interest in studying the impact of H₂S on the catalyst performance is due to its existence as an unavoidable byproduct from the HDS reaction. Overcoming or

* Corresponding author. Tel.: +81 92 802 2738; fax: +81 92 802 2792.

E-mail addresses: hamdy@chem-eng.kyushu-u.ac.jp, hamdy.farag@gmail.com (H. Farag).

neutralizing H_2S inhibition may allow for efficient catalytic HDS activity, especially for feedstocks of high sulfur content.

2. Experimental

2.1. The molybdenum sulfide phase

Molybdenum disulfide was synthesized by a high temperature annealing of ammonium tetrathiomolybdate ($(\text{NH}_4)_2\text{MoS}_4$) under application of 10 wt% H_2S in H_2 gas. A few grams of ammonium tetrathiomolybdate were placed in a silica boat and then loaded into a quartz tube. 10 wt% H_2S in H_2 gas was allowed to flow over the sample while applying a heating rate of $2^\circ\text{C}/\text{min}$ until 440°C . After the predetermined sulfidation time elapsed (ca. 8 h), the sample was flushed with argon gas for ca. 30 min. Argon gas was applied until the sample cooled to ambient temperature.

2.2. Characterization

The surface area was measured using a nitrogen adsorption isotherm at $\sim 196^\circ\text{C}$ on an automatic Micromeritics ASAP 2010C instrument. Before the sorption measurement, the sample was outgassed at 250°C for 12 h with a turbomolecular vacuum pump.

2.3. X-ray diffraction

X-ray powder diffraction was measured using a Rigaku Diffractometer with $\text{Cu K}\alpha$ radiation ($\lambda = 1.54056 \text{ \AA}$). The powder was loaded onto a glass disk and the diffractogram recorded with scan steps of 0.02° .

2.4. Scanning electron microscope (SEM)

All SEM micrographs were obtained using a Hitachi S-4700 field emission SEM. A specimen was set on carbon tape that was then fixed onto a copper sample holder and flushed with air. The sample holder was then attached to the SEM stub. The operating accelerating voltage was 30 kV.

2.5. Transmission electron microscopy (TEM)

Transmission electron microscopy (TEM) was used for lattice imaging to determine the textural properties of these nanoparticles. Images were obtained using a Hitachi 9000UHR at an accelerating voltage of 200 kV and at high resolution. A small fraction of these nanoparticles was dispersed in n-heptane (using a dilution factor of 5). A drop of the solution was spread over a copper grid that supported a thin film of amorphous carbon. The specimen was dried in air before analysis. The sample was cooled with liquid nitrogen before data collection.

2.6. Catalytic activity

The HDS reaction of DBT was carried out in a batch system using a 100 mL micro-autoclave reactor equipped with a sample withdrawal system. The sampling system was equipped with a stainless steel filter of ca. $1 \mu\text{m}$ sieve size. This assists in preventing the catalyst being removed from the system during the suction of samples. In a typical experiment, 10 mL of 1 wt% DBT solution in decane was loaded *in situ* into the reactor along with the freshly sulfided nanosized molybdenum disulfide catalyst (0.02–0.1 g). In some cases, fine copper powder (not quantitative) was included to mask the H_2S produced in the reaction. The reactor was purged several times with H_2 . The reaction pressure was eventually set at 3 MPa H_2 . During the reaction, small aliquots of less than 0.2 mL were withdrawn at various time intervals for analysis. Amounts of

each species produced in the reaction were determined using a gas chromatograph equipped with a flame ionization detector and a methylsiloxane capillary column ($0.32 \text{ mm} \times 50 \text{ m}$, HP6890). The identity of each species was determined using a gas chromatograph equipped with a mass spectrometer (HP5970). The effect of different H_2S partial pressures on the catalytic behavior for the DBT HDS system was studied. A wide variety of H_2S partial pressures were obtained after inserting either a predetermined amount of sulfur powder or a specific pressure of 10% (v/v) H_2S in H_2 gas mixtures into the feedstock. The amount of H_2S was determined using standard kits (GASTEC gas detector (Model SG 4010)) at the end of the reaction.

3. Results

3.1. Structure and morphology of the synthesized molybdenum disulfide

Fig. 1 shows the XRD pattern of the obtained MoS_2 after the thermal annealing of ammonium tetrathiomolybdate at 440°C . A relatively sharp (0 0 2) reflection (stacking direction) is observed along with peaks from other reflections. The spectrum was basically in agreement with that of the 2H- MoS_2 spectrum in JCPDS (number 6-97i) [19]. However, the (0 0 2) reflection in the XRD spectrum of our synthesized MoS_2 nanoparticles was characterized by a shift to a lower angle compared with the (0 0 2) reflection in the hexagonal 2H- MoS_2 crystals, i.e., a shift from $2\theta = 14.4^\circ$ (6.15 \AA) to $2\theta = 14.0^\circ$ (6.32 \AA). This indicates that the interlayer-distance of the MoS_2 layers may be larger. Annealing of MoS_2 nanoparticles can lead to a sharpening of the (0 0 2) XRD peak as the crystallinity of this phase is highly dependent on the manipulated temperature [20]. Heat treatment of ammonium tetrathiomolybdate in an environment of H_2S and using the present experimental conditions leads exclusively to the formation of a MoS_2 phase in which the Mo-to-S stoichiometric ratio is 1:2. This was ascertained by results from XRD as well as by elemental analysis. Fig. 2 shows a scanning electron micrograph of the MoS_2 product. Hexagonal agglomerates of anisotropic MoS_2 clusters can be seen. The hexagonal clusters are composed of several flakes. Cluster diameters vary in a broad range from 10 to a few tens of μm . The pores are probably located between the flakes because the outer surfaces of the clusters seem to be smooth. The nanosized MoS_2 sample possesses a BET surface area of $\sim 70 \text{ m}^2/\text{g}$ and an average pore size of $\sim 5 \text{ nm}$. The adsorption–desorption isotherm of this catalyst, Fig. 3, is typical for type IV from the conventional classification [21]. The desorption curve indicates a prevalence of mesoporosity in this sample. The intraparticle void may have partly contributed to the capillary phenomena. However, the median particle diameter as measured by the centrifugal sedimentation photo-extinction method using a SA-CP4L analyzer from Shimadzu Corp. was $1.5 \mu\text{m}$. Fig. 4 shows TEM images of the

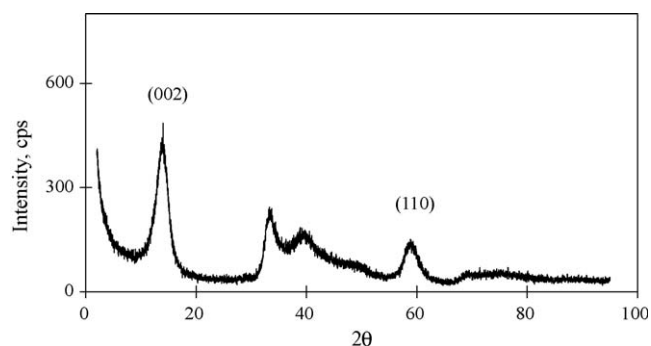


Fig. 1. XRD pattern of the synthesized nanosized MoS_2 .

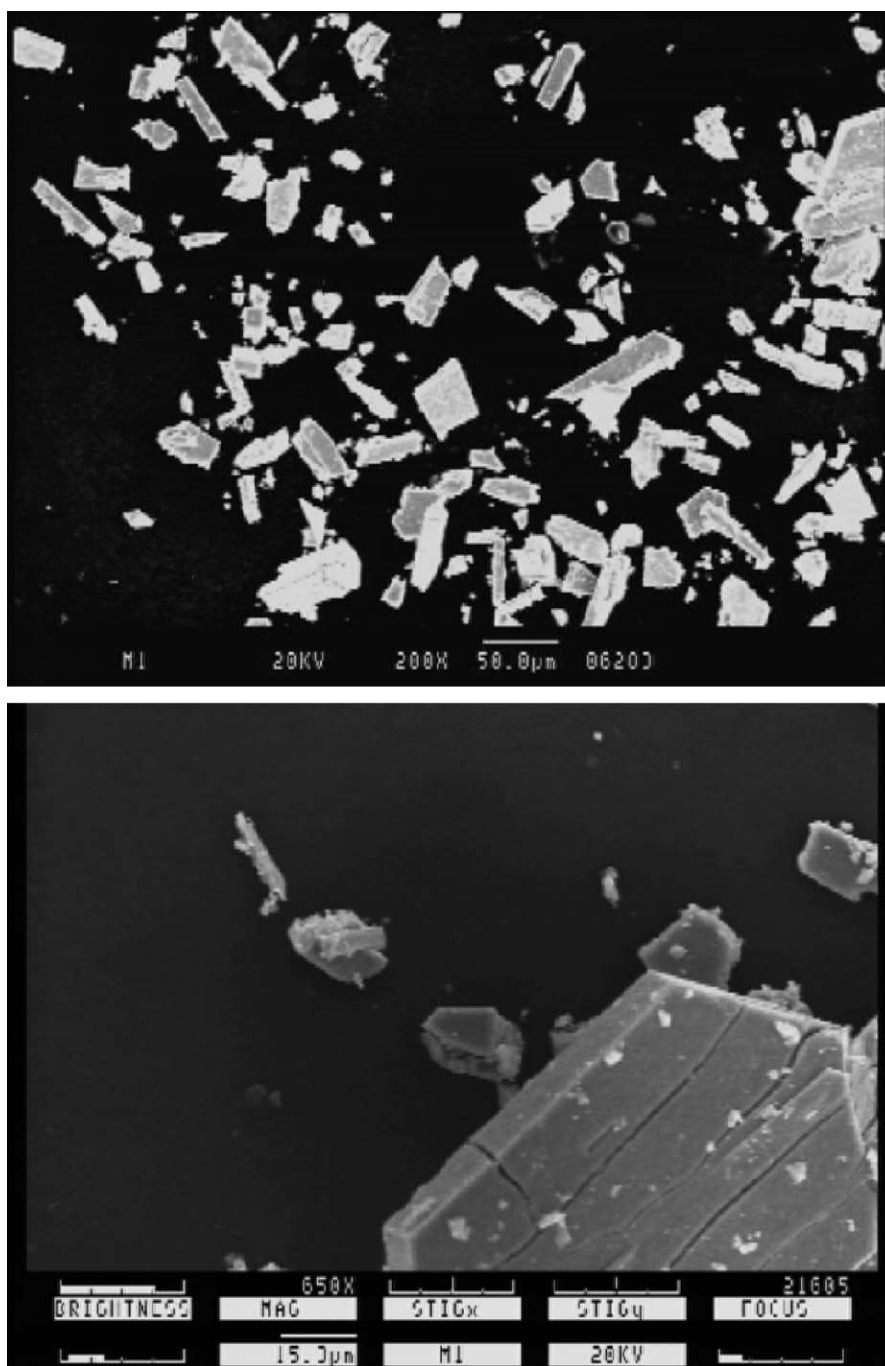


Fig. 2. SEM images of the synthesized nanosized MoS₂.

nanosized MoS₂. The nanosized MoS₂ was composed of layers with an interlayer-distance of ~ 0.632 nm, which is close to that determined by XRD. These nanosized MoS₂ layers are elongated and have a slab length of ~ 4.5 nm (calculated from the line broadening at the d-spacing of the (110) reflection). The crystallite size of nanosized MoS₂, as estimated from the line broadening at 2θ of 14.0 according to the method used in Ref. [9] was ~ 4 nm. However, it is interesting to note that the MoS₂ layers are mostly not straight but are bent to some extent.

3.2. Catalytic activity of the nanosized MoS₂ for the DBT HDS

The DBT HDS experiments over the nanosized MoS₂ catalyst were carried out at less than 3 MPa H₂ and at 340 °C and a small

amount of copper fine powder was included to serve as a H₂S scrubber. The HDS of DBT over the nanosized MoS₂ catalyst resulted mainly in the formation of bicyclohexyl, cyclohexylbenzene, biphenyl and 1,2,3,4-tetrahydro-dibenzothiophene. Trace amounts of partially hydrogenated dibenzothiophene species and isomers of bicyclohexyl and cyclohexylbenzene were also detected. The product identities are generally in agreement with that reported in literature [14,17,22,23]. The product distribution suggests that DBT HDS takes place through two parallel-consecutive reactions, namely a direct desulfurization and a hydrogenation reaction as shown in Scheme 1. The nature of the catalyst and the reaction matrices play important roles in determining the preferential reaction route in this scheme. In the HDS of DBT over the nanosized MoS₂ under the present

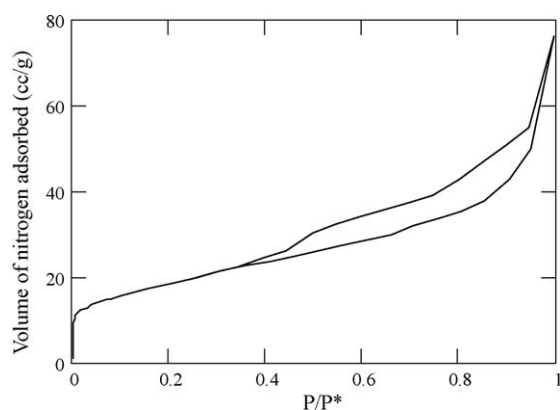


Fig. 3. Nitrogen adsorption-desorption isotherm for the synthesized nanosized MoS_2 .

conditions, the amount of product obtained from the hydrogenation pathway is comparable to that from the direct desulfurization route. Both these routes thus contribute substantially to the reaction.

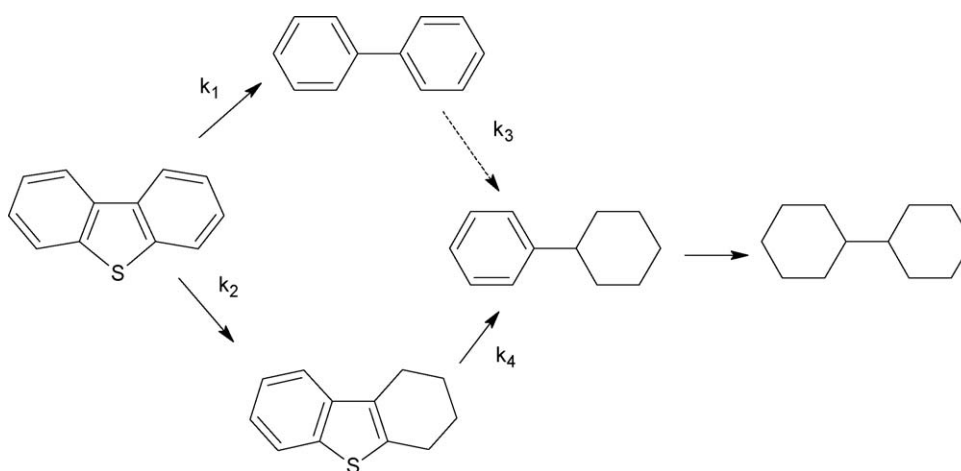
3.3. Impact of H_2S on the yield of DBT HDS products

The HDS of DBT over the present catalyst was investigated under different H_2S partial pressures, i.e., 13, 40 and 91 kPa. The influence of H_2S partial pressure on the catalytic performance in the DBT HDS can be assessed from the data set provided in Table 1. One may notice that at a H_2S partial pressure of 13 kPa, the overall catalytic activity increases sharply, i.e., the catalytic activity as expressed by the overall pseudo-first-order rate constant, Fig. 5, rose from ca. 9, the estimated value at low H_2S partial pressure, to ca. $25 \text{ s}^{-1} \text{ g}_{\text{cat}}^{-1}$, the value at 13 kPa H_2S . However, with a further increase in H_2S partial pressure, the catalytic activity first increased and then stabilized with almost no further change. The catalytic activity improved nearly seven times upon inclusion of H_2S as shown in Table 1. It is of interest to clarify how H_2S improves the catalyst activity. The catalyst before use was freshly sulfided and loaded *in situ* into the reactor. This manipulation excludes the possibility of the catalyst being partially oxidized and thus re-sulfided during the reaction. The remarkable increase in activity is attributed to the increased yield of the hydrogenation pathway. The yield of biphenyl at different levels of H_2S as a function of time in the DBT HDS is shown in Fig. 6. It is evident that only slight change in the biphenyl yield is obtained by including



Fig. 4. TEM image of the synthesized nanosized MoS_2 .

H_2S in the feedstock. The yield of lumped partially hydrogenated dibenzothiophene at various levels of H_2S as a function of time is shown in Fig. 7. It is noticeable that there is a steady upward shift in the maximum yield of these intermediates as the quantity of H_2S increases. The yields of bicyclohexyl and cyclohexylbenzene as well as their isomers resulted from the hydrogenation route. The yield of these products at different partial pressures of H_2S as a function of the reaction time is shown in Fig. 8. As the amount of H_2S increased the yield from the hydrogenation route increased markedly until a constant value was reached at a H_2S partial pressure of 91 kPa. The influence of H_2S on both activity and selectivity was proven experimentally to be reversible, i.e., in a reaction cycle we observed that keeping H_2S in the feedstock increases the catalytic activity while masking it reduces the activity. While the hydrogenation route products increase markedly when H_2S was present in the reaction zone, the direct desulfurization route products remained quantitatively almost unchanged.



Scheme 1. The DBT reaction network.

Table 1

Catalytic activity of the synthesized MoS₂ catalyst for the HDS of DBT investigated under a wide range of H₂S partial pressures.

	Partial pressure of H ₂ S, kPa			
	4	13.5	40.5	91
k_t^a	8.4	25.0 24.6 ^c	53.4 53.0 ^c	55.1
k_1^b	3.7	5.0	5.4	5.3
k_2^b	4.7	20.0	48.0	51.7
k_3^b	<0.01 ^d	1 ^d	<0.01 ^d	<0.01 ^d
k_4^b	105	108	108	108
k_2/k_1 (selectivity)	1.3	4.2	8.9	9.7
H ₂ S/H ₂ mole ratio	4.5×10^{-3}	9.0×10^{-3}	2.6×10^{-2}	3.7×10^{-2}

^a Apparent total pseudo-first-order rate constant, $\times 10^{-4} \text{ s}^{-1} \text{ g}_{\text{cat}}^{-1}$.

^b Apparent individual rate constants according to Scheme 1.

^c Cycled test results.

^d Tentative.

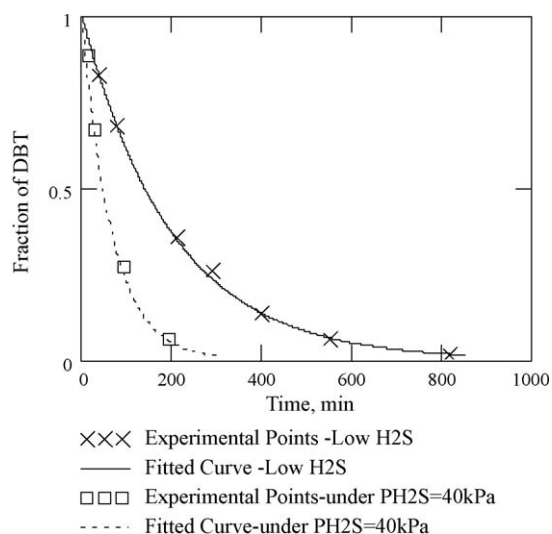


Fig. 5. Pseudo-first-order plots of the DBT HDS for different concentrations of H₂S in the feedstock.

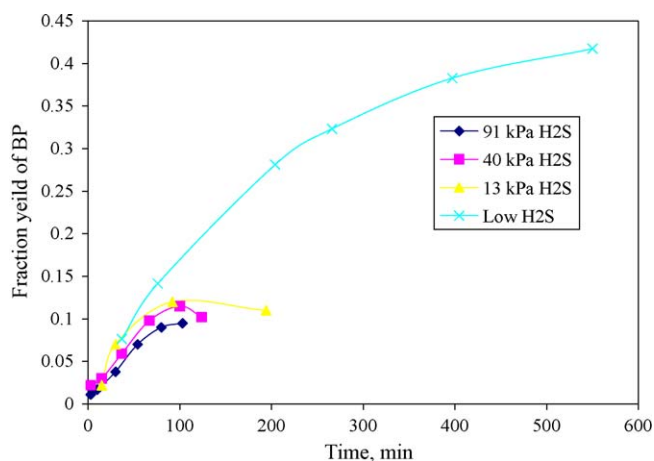


Fig. 6. The fraction yield of biphenyl (BP) isomers versus reaction time at various pressures of H₂S in the HDS of DBT.

4. Discussion

4.1. Characterization of nanosized MoS₂

Despite the MoS₂ structure having been thoroughly studied, many recent studies have been undertaken [24–27]. This shows

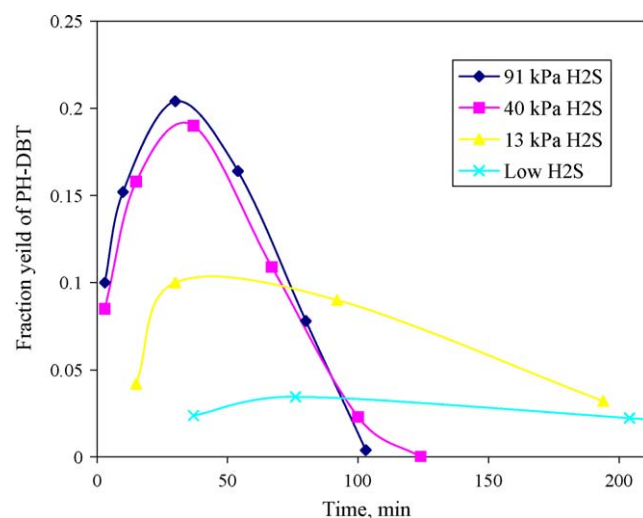


Fig. 7. The fraction yield of partially hydrogenated dibenzothiophenes (PH-DBT) versus reaction time at various pressures of H₂S in the HDS of DBT.

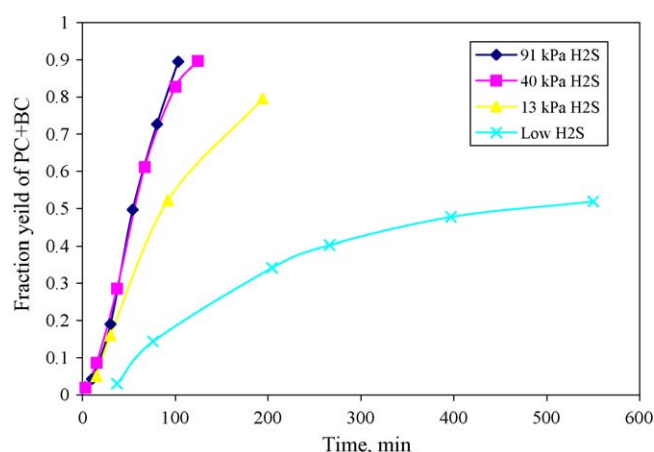


Fig. 8. The fraction of the lumped yield of bicyclohexyl (BC), cyclohexylbenzene (PC) and their isomers versus reaction time at various pressures of H₂S in the HDS of DBT.

that nanoscale MoS₂ is widely applied from potential utilization in nanoelectronics to heterogeneous catalysis, which is the essential motivation our studies. The layered structure of MoS₂, for instance, allows application in various fields such as in lubrication and sensors. Optical and chemical properties of the MoS₂ are claimed to be size dependent. Bulk MoS₂ exhibits a narrow optical absorption band; however, nanoscale MoS₂ clusters exhibit a wide optical absorption band [25]. Lauritsen et al. [27] have recently observed several structural transitions that correlate to the size of MoS₂ nanocrystals. They further have found that the edge structure of these nanocrystals is dependent on the actual size of the clusters. Accordingly, important effects on the catalytic behavior of these materials may be expected. The chemical structure of the species is typical of MoS₂ with a Mo:S atomic stoichiometric ratio of about 1:2. However, this phase may appear in various morphologies. The obtained species evidently formed hexagonal clusters. The average number of stacked MoS₂ layers was ca. 6. However, the average slab length (basal plane) of these layers was estimated to be ~4.5 nm. A shift of the hexagonal 2H-MoS₂ (0 0 2) reflection XRD peak from its standard position along with its broadening clearly indicates that the MoS₂ layers are curved. This was further supported by TEM images as shown in Fig. 4. It is interesting that many agglomerates are present in which most of the MoS₂ layers

are bent to a certain extent. The agglomerates are parabolic batches of MoS₂ layers and mostly have a uniform size. The morphology of each batch is characterized by a stack of MoS₂ layers in which the inner and the outer core layers have different morphology, i.e., MoS₂ layers in the outer core are characterized by a slab length longer than those in the inner core as shown in Fig. 4. Therefore, the inner elliptical layers may experience more strain than the outer layer. Furthermore, the outer elliptical layers may not be fully commensurate with the structure of the inner elliptical layers. The bent layers of MoS₂ are probably associated with the formation of defects, i.e., unsaturated active sites and these are considered crucial for catalytic and other properties [28,29]. Each MoS₂ layer in these batches may experience strain and this is different to the strain on other layers. Consequently, we propose that each MoS₂ layer has a distinct surface (basal) and edge structure. The upward shift in average distance between the layers of the present nanosized MoS₂ from 0.615 nm, the value for the hexagonal 2H-MoS₂ bulk phase, to 0.632 nm as determined from the XRD pattern (Fig. 1) is presumably attributed to the curve feature of the layers. This curvature of the MoS₂ layers has been reported to be related to the annealing temperature, i.e., as the temperature of annealing increases the curvature of the layers increase to the extent that even closed MoS₂ layers may be formed [30].

4.2. Catalytic properties

The MoS₂ phase is of great interest as a catalyst in HDS reactions. The importance of nanoscale MoS₂ as a catalyst lies not only in its relatively high activity, which for a given process is not be so higher than other metallic derivatives, but in its behavior towards the reaction matrices. To gain more insight into the nature of the DBT HDS reaction over this catalyst, the reaction kinetics was investigated at specific time intervals. The batch reactor allows us to follow up on the details of reaction pathways and thus enables the setting up of a proper reaction scheme. DBT HDS reactions over the nanosized MoS₂ catalyst fitted reasonably well with pseudo-first-order kinetics and this is in agreement with other studies [13,29], Fig. 5. However, there is no generally accepted description of detailed kinetics of this consecutive-parallel system in the literature. Most studies use a numerical solution to estimate the relative rate constants in these schemes [17,22,23]. Results obtained from this treatment are, however, mostly tentative. In a recent study [31], it was shown that the relative contributions of the direct sulfur extraction route (k_1) and the hydrogenative desulfurization route (k_2) in the HDS reaction of DBT can be confused unless one clearly knows the values of subsequent hydrogenation pathways (k_3 and k_4). Furthermore, a proper solution for estimating the rate constants in this scheme is suggested.

Figs. 9 and 10 show experimental results from the transformation of DBT as a function of time fitted with the curves theoretically estimated according to the proposed models described in Ref. [31] for a similar system. Reasonable matches between experimental results and theoretical data are obtained. This kinetic treatment enables us to properly estimate all the individual rate constants as shown in Scheme 1.

The order of the DBT HDS with respect to H₂S is estimated according to the following equation:

$$R = \frac{\partial C_{DBT}}{\partial t} = k^o [C_{DBT}] [P_{H_2S}]^n \quad (1)$$

where C_{DBT} is the concentration of DBT at certain reaction time, R is the rate of the reaction per gram of catalyst at C_{DBT} , k^o is the reaction rate constant, P_{H_2S} is the partial pressure of H₂S, and n is order of the reaction with respect to H₂S. At a fixed conversion level

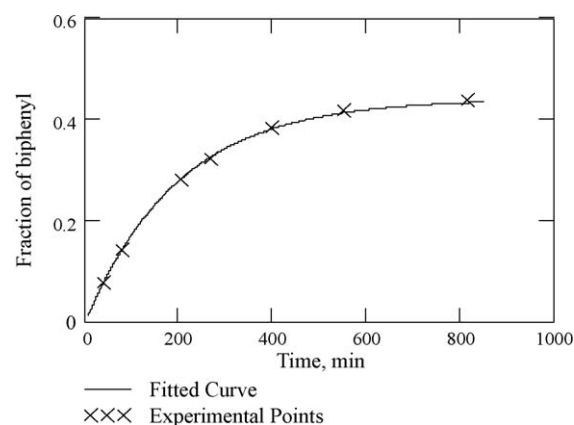


Fig. 9. Experimental points for the fraction of lumped biphenyl isomers as a function of reaction time in the DBT HDS over the nanosized MoS₂ catalyst matched with the kinetic model (low H₂S in the feedstock).

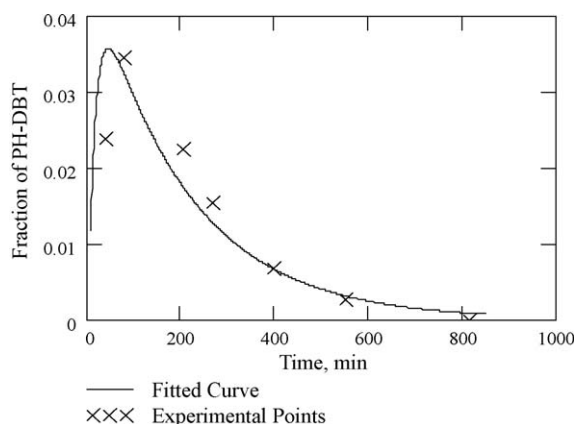


Fig. 10. Experimental points for the fraction of lumped PH-DBT species as a function of reaction time in the DBT HDS over the nanosized MoS₂ catalyst matched with the kinetic model (low H₂S in the feedstock).

of the substrate, the term $k^o [C_{DBT}]$ is constant and Eq. (1) simplifies to:

$$R = k^* [P_{H_2S}]^n \quad (2)$$

The rate, R , was estimated from the slope of the tangent line at a certain conversion level of DBT from the graph of the DBT concentration–time function. Fig. 11 demonstrates the plot of $\ln R$ versus $\ln P_{H_2S}$ at a steady DBT conversion of ~73%. The order of the reaction with respect to H₂S as estimated from this plot and under the present experimental conditions was +0.14. The positive order of H₂S is an indication of the positive impact of H₂S on the catalytic activity. The greatest enhancement in activity results from an increase in the yield of product formed via the hydrogenation pathway. Nevertheless, the yield of product formed from the direct desulfurization route showed no significant change. The process was experimentally assured to be reversible, i.e., typical results were observed on testing the catalyst in a repeated reaction cycle with different H₂S levels. This may indicate that the interaction between H₂S and potential active sites is a physical phenomenon. It may further indicate the stability of the nanosized MoS₂ active phase when investigated under H₂S partial pressures in the range of 13–91 kPa. These results obviously support the notion of the existence of two different active sites, one for direct sulfur extraction and the other for hydrogenation. Our results clearly show that the hydrogenation active site is in fact subject to promotion by H₂S.

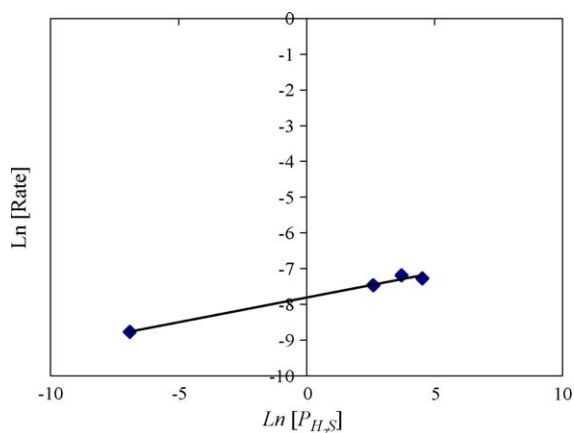


Fig. 11. Plot for estimating the order of the DBT HDS with respect to H_2S ; R is the rate of the reaction at a DBT conversion of 73% and P_{H_2S} is the partial pressure of H_2S expressed in kPa.

Table 1 summarizes kinetic results of the DBT HDS reaction under different conditions. The direct sulfur extraction route (k_1) did not suffer any inhibition by H_2S as the apparent rate constant, k_1 , hardly changed with a variation in H_2S partial pressure. The desulfurization apparent rate constant of the partially hydrogenated DBT is remarkably higher than the overall apparent rate constant of the parent substrate or other individual apparent rates as shown in Scheme 1 and Table 1 by comparing the value of k_4 to other apparent rate constant values. This high rate remains independent on the presence or absence of H_2S in the feedstock. The identity of this intermediate is distinctly different from the parent DBT in terms of molecular geometry. The breakdown of the plane symmetry of these intermediates enables them to easily access active sites and consequently make them more reactive than the DBT parent substrate. Moreover, as the concentration of H_2S increased the maximum yield of H4-DBT also increased with a stepwise shift towards a lower reaction time, Fig. 7. This can be interpreted by comparing the rate constants that are attributed to the reaction of this intermediate. While the rate constant of the hydrogenation reactions, k_2 , increased with H_2S concentration, k_4 values remained independent of H_2S in the reaction. The high yield obtained from the hydrogenation route is very beneficial in overcoming the steric hindrance limitation of this substrate.

It is interesting and yet astonishing to observe that these nanosized MoS_2 particles effectively catalyze DBT HDS in the presence of H_2S . The crystal size range of 4–5 nm for the nanoscale MoS_2 seems to exert a specific catalytic performance irrespective of the synthetic origin of the catalyst. Furthermore, these MoS_2 clusters promote the HDS reaction preferentially and mainly via the hydrogenation route. By considering this catalyst's selectivity, process options may be considered. These nanoscale MoS_2 catalysts are worthwhile in terms of HDS activity and also in their response to reaction matrices, especially those containing H_2S . Smaller sized catalysts and larger sized catalysts than those studied have been subject to inhibition by H_2S [12]. For smaller sized MoS_2 clusters, a relatively large percentage of atoms are located on the surface. Active sites are thought to be the unsaturated sites located on the edges of the catalyst surface. It is thus expected that for the nanosized MoS_2 studied in this work a different morphology and thus catalytic performance would be obtained. In HDS over conventional NiMo- and/or CoMo-based catalysts, H_2S greatly reduces the overall activity [32,33]. Accordingly, it is often considered as a serious inhibitor for this class of catalyst. In this instance, the active sites that are anchored with H_2S are more likely catalytically inactive. In other words, some active sites may be excluded from participating in the activity,

which results in a reduction of the number of potentially active sites. Such inhibition by H_2S has also been reported for supported and unsupported MoS_2 catalysts [11,12,34,35]. On the other hand, in HDS over the present nanoscale MoS_2 catalysts, H_2S greatly improves the overall catalytic activity. However, the optimum catalytic HDS activity seems to be associated with a certain size of MoS_2 . As the nanoscale size of MoS_2 changes, the edge structure also changes. Accordingly, the catalytic activity and responses to reaction matrices may also change. Potentially active sites in the presence of H_2S may be different from the well-known rim, edge and brim sites. A certain cluster size of MoS_2 may be essential for the H_2S -modified active sites to be positively and efficiently used in the HDS reaction.

4.3. Promotion versus inhibition

H_2S exerts a substantial inhibitive effect in the HDS reaction over NiMo- and CoMo-based catalysts as well as over unsupported MoS_2 catalysts, even when present in very small amounts. The coexistence of H_2S in the HDS reaction causes a dramatic change not only in catalyst activity but also in reaction selectivities. With H_2S in the feed, the overall activity is lowered by an order of magnitude in the early stages of the HDS reaction [33,34]. In the HDS of polyaromatic thiophenes over conventional catalysts, it is well known that H_2S exerts a dramatic detrimental effect on the direct desulfurization route and only a slight influence on the hydrogenation pathway. Therefore, the deterioration in activity is mainly a result of a lower yield from the direct desulfurization route. This may explain why individual refractory sulfur compounds undergo different degrees of inhibition by H_2S . It seems probable that H_2S may mask and/or modify potential sites for direct desulfurization so that they will not be catalytically effective. The blockage and thus loss of these potentially active sites would result in a serious decrease in overall catalyst activity, especially for substrates that prefer the direct sulfur extrusion reaction. The assumption that two distinct active sites exist principally originates from this evidence. It is interesting to note that the effect of H_2S , regardless of whether it acts as an inhibitor or an enhancer in the HDS of DBT reaction, is readily reversible. This may infer that H_2S causes no permanent change in the catalyst structure. In the HDS over conventional CoMo- and NiMo-based catalysts, it has been reported that the activity decreased as the H_2S concentration in the feedstock increased until a specific concentration level above which H_2S exerts no further influence on the overall activity. To the best of our knowledge, the presence of H_2S in HDS reactions has never been reported to completely deactivate the catalyst. This means that not all the potentially active sites are subject to masking or blocking by H_2S . In other words, H_2S only partially affects the catalyst activity.

On the other hand, H_2S exerts a significant positive effect in HDS when a certain size of nanosized MoS_2 catalysts is used. The nanosized MoS_2 catalyst used in our study is such an example. This can be easily recognized from the positive order of H_2S , i.e., +0.14, as determined from Fig. 11. Fig. 12 shows a comparison of the product yields in the presence and absence of H_2S in the feedstock at a DBT conversion of 73%. Our results reveal that while the yield from the hydrogenation pathway is greatly increased by the presence of H_2S , the yield from the direct desulfurization route underwent a considerable reduction at a H_2S partial pressure of 13 kPa. At higher partial pressures of H_2S , only subtle changes in the yield from the direct desulfurization route, i.e., (BP) was observed. This indicates that H_2S mainly modifies the hydrogenation active sites through specific interactions. Thus, it is probably not only the number of active sites that governs catalyst activity but also the intrinsic activity of these modified sites. These results clearly show that the hydrogenation site is in fact subject to

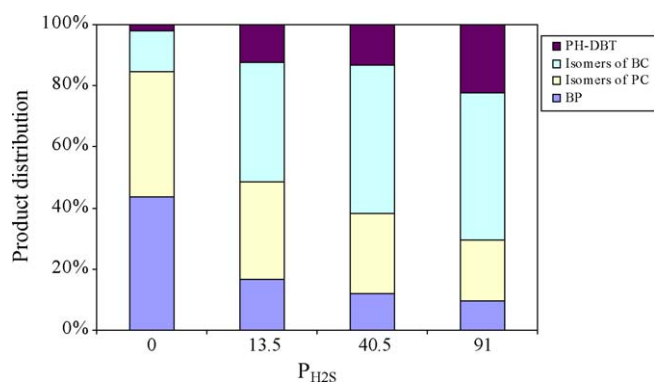
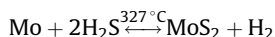


Fig. 12. The effect of H₂S on product distribution after DBT HDS at a conversion of ~73%. *BC, bicyclohexyl isomers. *PC, cyclohexylbenzene isomers. *BP, isomers of biphenyl. *PH-DBT, partially hydrogenated-dibenzothiophenes.

promotion by H₂S. In this case, H₂S had to remain intact until it reached the catalyst's potential active sites. This interaction creates sites that may or may not be of considerable catalytic efficacy. The catalytic properties of the nanosized MoS₂ used in this study are closely related to the structural properties of its surface.

It is important to discuss the present results in terms of the possible artifacts related to these experiments. It may be argued that under low H₂S partial pressure, the catalyst undergoes a reduction that leads to a Mo metal phase while on increasing the partial pressure of H₂S the formation of more molybdenum sulfide takes place [36]. This might partly explain the results as the activity of the Mo metal phase is much lower than that of the molybdenum sulfide phase [37]. However, this assumption is contradicted by the thermodynamic results associated with the reduction in the equilibrium of MoS₂. Thermodynamic data shows [38] that the H₂S/H₂ equilibrium ratio for the following reaction:



at 327 °C is 4×10^{-7} . Therefore, it would be expected that the stability of the MoS₂ phase increases with an increase in the H₂S/H₂ ratio above this value. The H₂S/H₂ ratios used in the HDS of DBT over the present catalyst are listed in Table 1. The applied H₂S/H₂ ratios are thousands of times higher than the equilibrium ratio even at the lowest partial pressure of H₂S. The MoS₂ catalyst will thus not be reduced as shown by the thermodynamic data. Accordingly, under the stated reaction conditions, the Mo phase presumably exists in a completely sulfided form.

The constant catalyst activity at high concentrations of H₂S (Table 1) suggests that the effect of H₂S on the activity is not simple. Therefore, some interesting points can be discussed. When the H₂S concentration is high enough to saturate the active sites on

the catalyst surface then no further effect of excess H₂S on the activity is expected. H₂S strongly inhibits the HDS reaction over conventional catalysts and at higher concentrations of H₂S the degree of inhibition remains constant. It appears that potentially active sites are varied and only a certain type of site undergoes either promotion or inhibition by H₂S. A saturation state is reached when all the potential active sites, which are subject to modification by H₂S, have been consumed. This indicates that the catalyst inhibition and/or promotion by H₂S are limited at this saturation level.

4.4. Role of MoS₂ bent layers in activity and selectivity

The MoS₂ synthesized in this study is characterized by bent MoS₂ layers. The curvature of the layer seems to be important for the exploration of its novel catalytic performance because of the defects in the atomic surface structure. As shown in Table 1, the reaction rate increases linearly with increasing H₂S partial pressure in the feed until it becomes constant. The outer core of the bent basal plane may participate in the activity along with the inner core as shown in Fig. 13. In addition, these bent layers facilitate the hydrogenation route, especially when the HDS reaction takes place in the presence of H₂S. Complete round and/or straight MoS₂ layers may be argued to possess limited activity because their basal planes are catalytically inert. The catalytic behavior of the MoS₂ layers is probably sensitive to the extent of their bending. We assert that the curved layers of MoS₂ demonstrate specific interactions with the reaction matrices. This study has showed that HDS activity of the nanoscale MoS₂ of ca. 4 nm in size is significantly improved in the presence of H₂S. MoS₂ particles of similar cluster size have been reported to exhibit electronic and optical properties that are entirely different from those of the bulk MoS₂ phase [2]. The catalytic activity of nanoscale MoS₂ is thus a size dependent phenomenon. The production of a number of isomers in the HDS of DBT may be attributed to the acidity (–SH group) of the catalyst which results from the interaction of H₂S with the catalyst surface. A similar positive effect by H₂S on the activity of supported and unsupported nanosized Cr₂S₃ and Co₉S₈ catalysts has been reported for the hydrogenation reaction of toluene [38]. This behavior has been argued to increase the –SH concentration (Bronsted sites) on the catalysts. The isomers observed after the DBT HDS reaction in this study may thus be attributed to the presence of considerable catalytic acidity. The bending of MoS₂ nanoslabs may affect the catalyst acidity which can be further developed with the coexistence of H₂S. Practically any catalyst involved in the HDS operates under an environment of H₂S where it usually significantly decreases catalytic activity. Accordingly, the fact that the studied nanosized MoS₂ are active in the presence of H₂S is advantage and can be exploited. In the

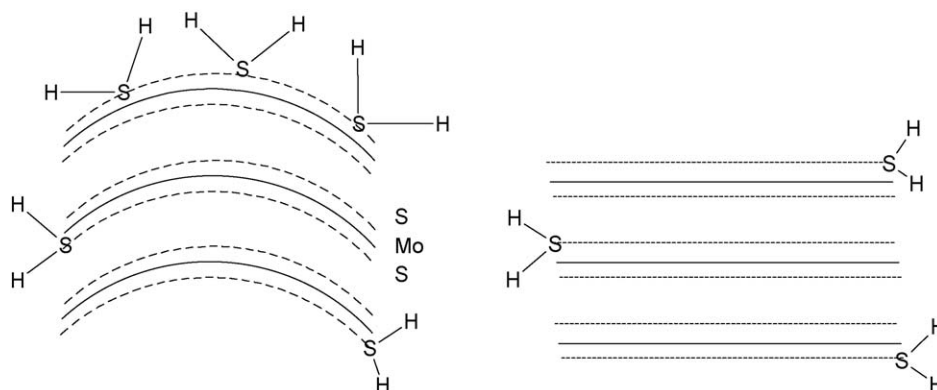


Fig. 13. Model for H₂S interaction with bent- and straight-like MoS₂ layers.

absence of H₂S the ratio of k_2/k_1 , which represents the selectivity, was close to unity while it was much higher than unity in the presence of H₂S. In this case, the DBT HDS reaction was greatly favored by aromatic ring hydrogenation. This indicates that HDS reaction pathways may be controlled by using a relevant nanosized MoS₂ catalyst. Therefore interesting consequences for the development of catalytic activity is viable.

5. Conclusions

MoS₂ catalysts with a size of ca. 4 nm showed interesting catalytic performance. The synthesized nanosized MoS₂ catalyst consists of separate batches of bent MoS₂ layers of ca. 4 nm size. The nanosized MoS₂ catalyst exhibits completely new behavior since its activity for the DBT HDS reaction is dramatically enhanced in the presence of H₂S. In contrast to the behavior of the classic Mo-, CoMo- or NiMo-based catalysts that suffer severe inhibition by the presence of H₂S in the HDS feedstock, the activity of the synthesized nanosized MoS₂ catalyst improved significantly in its presence. This finding indicates that H₂S interacts with potential active sites resulting in new sites that showed a distinct activity. The textural property of the synthesized MoS₂ is a key factor that determines whether these newly created sites are catalytically important. We argue that the positive influence of H₂S in the HDS of DBT may be a consequence of the curved structure of MoS₂ layers. In the presence of H₂S, the DBT HDS mainly occurred via the hydrogenation pathway and the contribution from the direct sulfur extraction route was minimal.

In essence, the following main points may summarize the effect of H₂S on the catalysis of HDS:

1. H₂S inhibits the HDS activity of Mo-, NiMo- and CoMo-based catalysts.
2. H₂S results in a dramatic change in HDS selectivity.
3. H₂S never completely deactivates the catalyst.
4. The activity changes, whether increasing (promotion) or decreasing (inhibition), is a function of H₂S concentration until a saturation state is reached wherein H₂S has no more impact on the activity.
5. H₂S may act as a promoter or as an inhibitor depending on the identity of the catalyst.
6. The mechanism of H₂S when behaving as an inhibitor or as a promoter is proposed to be of similar origin.
7. MoS₂ layers with a specific curvature are presumably necessary for H₂S to act as an activity enhancer for the catalyst.

References

- [1] R.R. Chianelli, M. Daage, M.J. Ledoux, *Adv. Catal.* 40 (1994) 177–232.
- [2] B.L. Abrams, J.P. Wilcoxon, *Crit. Rev. Solid State Mater. Sci.* 30 (3) (2005) 153–182.
- [3] V.N. Bakunin, A.Y. Suslov, G.N. Kuzmina, O.P. Parenago, *J. Nanoparticle Res.* 6 (2–3) (2004) 273–284.
- [4] P.D. Fleischauer, *Thin Solid Films* 154 (1987) 309–322.
- [5] E. Comini, V. Guidi, M. Ferroni, G. Sberveglieri, *IEEE Sens. J.* 5 (1) (2005) 4–11.
- [6] J. Janata, M. Josowicz, P. Vanysek, D.M. DeVaney, *Anal. Chem.* 70 (12) (1998) 179R–208R.
- [7] J. Chen, F. Wu, *Appl. Phys. A: Mater. Sci. Process.* 78 (7) (2004) 989–994.
- [8] H.C. Woo, I.S. Nam, J.S. Lee, J.S. Chung, Y.G. Kim, *J. Catal.* 142 (2) (1993) 672–690.
- [9] H. Farag, K. Sakanishi, M. Kouzu, A. Matsumura, Y. Sugimoto, I. Salto, *J. Mol. Catal. A: Chem.* 206 (1–2) (2003) 399–408.
- [10] H. Farag, K. Sakanishi, *J. Catal.* 225 (2) (2004) 531–535.
- [11] H. Farag, K. Sakanishi, M. Kouzu, A. Matsumura, Y. Sugimoto, I. Salto, *Catal. Commun.* 4 (7) (2003) 321–326.
- [12] H. Topsoe, *Appl. Catal. A: Gen.* 322 (2007) 3–8.
- [13] I. Mochida, K. Choi, *J. Jpn. P. I.* 47 (3) (2004) 145–163.
- [14] S.P. Kelty, G. Berhault, R.R. Chianelli, *Appl. Catal. A: Gen.* 322 (2007) 9–15.
- [15] N. Elizondo-Villarreal, R. Velazquez-Castillo, D. Galvan, Structure and catalytic properties of molybdenum sulfide nanoplatelets, *Appl. Catal. A: Gen.* 328 (1) (2007) 88–97.
- [16] D.D. Whitehurst, T. Isoda, I. Mochida, *Adv. Catal.* 42 (1998) 345–471.
- [17] N. Guernalec, T. Cseri, P. Raybaud, C. Geantet, M. Vrinat, *Catal. Today* 98 (2004) 61–66.
- [18] M.C. Kerby, T.F. Degnan Jr., D.O. Marler, J.S. Beck, *Catal. Today* 104 (2005) 55–63.
- [19] JCPDS (Joint Committee for Powder diffraction Studies), International Center for Diffraction Data, Swarthmore, PA, 1986.
- [20] X. Lin, Y. Li, *Chem. Eur. J.* 9 (2003) 2726–2731.
- [21] S.J. Gregg, K.S.W. Sing, *Adsorption, Surface Area, and Porosity*, 2nd edition, Academic Press, London, 1982.
- [22] M. Daage, R.R. Chianelli, *J. Catal.* 149 (2) (1994) 414–427.
- [23] C.T. Tye, K.J. Smith, *Catal. Today* 116 (2006) 461–468.
- [24] T.R. Thurston, J.P. Wilcoxon, *J. Phys. Chem. B* 103 (1999) 11–17.
- [25] D.F. Kelley, V. Chikan, *J. Phys. Chem. B* 106 (2002) 3794–3804.
- [26] S. Gemming, G. Seifert, *Nat. Nanotechnol.* 2 (2007) 21–22.
- [27] J.V. Lauritsen, J. Kibsgaard, S. Helveg, H. Topsoe, B.S. Clausen, E. Laegsgaard, F. Besenbacher, *Nat. Nanotechnol.* 2 (2007) 53–58.
- [28] T. Weber, J.C. Muijsers, J.H.M.C. van Wolput, C.P.J. Verhagen, J.W. Niemantsverdriet, *J. Phys. Chem.* 100 (1996) 14144–14150.
- [29] Y. Iwata, K. Sato, T. Yoneda, Y. Miki, Y. Sugimoto, A. Nishijima, H. Shimada, *Catal. Today* 45 (1998) 353–359.
- [30] Y. Feldman, G.L. Frey, M. Homyonfer, V. Lyakhovitskaya, L. Margulis, H. Cohen, G. Hodes, J.L. Hutchison, R. Tenne, *J. Am. Chem. Soc.* 118 (1996) 5362–5367.
- [31] H. Farag, *Energy Fuels* 20 (2006) 1815–1821.
- [32] V. Rabarihoela-Rakotovo, S. Brunet, G. Perot, F. Diehl, *Appl. Catal. A: Gen.* 306 (2006) 34–44.
- [33] S.T. Sie, *Fuel Process. Technol.* 61 (1–2) (1999) 149–171.
- [34] E.O. Orozco, M. Vrinat, *Appl. Catal. A: Gen.* 170 (2) (1998) 195–206.
- [35] E. Lecrenay, K. Sakanishi, T. Nagamatsu, I. Mochida, T. Suzuka, *Appl. Catal. B* 18 (1998) 325–330.
- [36] K. Soni, B.S. Rana, A.K. Sinha, A. Bhaumik, M. Nandi, M. Kumar, G.M. Dhar, *Appl. Catal. B* 90 (2009) 55–63.
- [37] E.J.M. Hensen, H.J.A. Brans, G. Lardinois, V.H.J. de Beer, J.A.R. van Veen, R.A. van Santen, *J. Catal.* 192 (2000) 98–107.
- [38] N. Guernalec, C. Geantet, P. Raybaud, T. Cseri, M. Aouine, M. Vrinat, *Oil Gas Sci. Technol.* 61 (2006) 515–525.